

Anti-atrazine Functionalized Gold-nano Structures for Environmental Monitoring

Anu Singh^{1,2}, Yuvraj Joshi¹, Meenakshi Choudhary¹, Manoj Pratap Singh¹ and Kavita Arora^{1*}

¹Advanced Instrumentation Research Facility, Jawaharlal Nehru University, New Delhi-110067, India

²Department of Biotechnology, School of Life Sciences, Jaipur National University, Jaipur, Rajasthan, India

Abstract

Atrazine, a pesticide is a xenobiotic compound known to be a putative endocrine disruptor that may cause serious health risks even at very low levels. As per World Health Organization (WHO) the permissible limit of atrazine is restricted to 2 $\mu\text{g L}^{-1}$ in drinking water and 0.02 -15 ppm (mg L^{-1}) in food and it has been classified as Class 3a carcinogen as per IARC 2001. We report application of anti-atrazine based immune sensor for detection of atrazine using directly deposited gold nanostructures onto ITO glass slides for environmental monitoring. Non-toxic, simple and directly deposited gold nano structures (GNS-ITO) were characterized using cyclic voltammetry and UV visible absorption that showed characteristic absorption peak at ~ 559 nm confirming presence of 20-30 nm sized nano-structured hexagonal humps. Anti-atrazine has been covalently immobilized onto GNS-ITO and characterized using FT-IR spectroscopy, CV and SEM. Interestingly, SEM images reveals that the GNS grown on the surface are spherical and symmetrically distributed throughout the surface. Fabricated immune electrodes were used to sense atrazine through Square Wave Voltammetry and it was found to have dynamic linear range from 50 aM - 1 nM (10.78 fg mL^{-1} - 215 pg mL^{-1}) in 60 s antigen exposure time. Fabricated immune electrode was also shown to retain substantial stability till 12 weeks upon storage at 4°C in desiccated condition and showed no binding with non-specific antigens like malathion, parathion, 2-amino anthracene, albendazole etc. This system offers the potential for rapid, cost-effective immunosensing for the analysis of samples of environmental, medical and pharmaceutical significance.

Keywords: Atrazine; Immunosensor; Gold-nano-structures; Pesticides; Environmental monitoring

Introduction

Wide use of pesticides/herbicides/insecticides to combat increasing needs of society has imposed a serious threat to environment and public health. A pesticide is any substance or mixture of substances intended for preventing, destroying, repelling, or mitigating any pest. Pesticide can be chemical substance, biological agent, antimicrobial, disinfectant or device [1]. The effect of this chemical substance is wide-ranging even when it is applied on a small area. It spreads through air, seeps in the soil or dissolves in the water, and eventually reaches a larger area. Agricultural production is currently, and increasingly, dependent on the use of pesticides. Pesticides often seep into ground water, which is consumed by humans, consequently poisoning them over a period of time. Animals and humans are leading towards very serious illnesses and deaths by consuming residual pesticides present in plants. Detection of pesticides is therefore highly desired both in case of food and water quality control or environmental monitoring. Some of the generally used pesticides are Atrazine, Bensulide, 2,4-D, DSMA, Dacthal, Dicamba, Diquat Dibromide, Endothall, Glyphosate, Isoxaben, MCPA, MCPP, MSMA, Pendimethalin, Prometon, Pronamide, Siduron, Triclopyr, Trifluralin. Among these Atrazine (2-chloro-4-ethylamino-6-isopropyl-amine-s-triazine) is widely used synthetic herbicide throughout the world [2] to control broadleaf and grassy weeds [3]. Atrazine is used on crops such as sugarcane, corn, pineapples, sorghum, and macadamia nuts, and on evergreen tree farms and for evergreen forest regrowth. It has also been used to keep weeds from growing on both highway and railroad rights-of-way. Atrazine can be sprayed on croplands before crops start growing and after they have emerged from the soil. Some of the trade names of atrazine are Aatrex®, Aatram®, Atratol®, and Gesaprim®. The scientific name for atrazine is 6-chloro-N-ethyl-N'-(1-methylethyl)-triazine-2,4-diamine. Atrazine is regarded as one of the important pollutant of environmental concern listed in top 20 of 1636 in NPL (National

Priority List) by EPA due to its low biodegradability and its high potential to contaminate the surface waters and ground water [4]. Presence of atrazine at ppb level has shown to disrupt the sexual development in amphibians and thus may pose serious ecological risks. World Health Organization (WHO) has suggested the permissible limit is restricted to 2 $\mu\text{g L}^{-1}$ in drinking water and 0.02 - 15 ppm (mg L^{-1}) in food [5]. As per EPA/ WHO Atrazine is a class 3a toxicant (<http://monographs.iarc.fr/ENG/Monographs/vol73/volume73.pdf>), which is highly toxic to humans and other animals. It can reach to blood stream through oral, dermal and inhalation exposure, which can cause pain, diarrhea and vomiting, eye irritation, irritation of mucous membrane and possible skin reactions [5]. It also shows effects on reproduction, teratogenic effect, [6] mutagenic effect [6,7] carcinogenic effect [6,7] organ toxicity [7]. Therefore, it is of great significance to accurately monitor and quantify atrazine at low concentrations in various environmental samples. Conventionally, atrazine is detected and quantified using high-performance liquid chromatography (HPLC) with UV-Visible detection [8], liquid chromatography-mass spectrometry and gas chromatography coupled to various detectors like flame ionization, electron capture, mass spectrometry [9], enzyme linked immunosorbent assay [10,11], etc. Atrazine has been shown to be detected upto 0.1 $\mu\text{g L}^{-1}$ using GC/MS method, 0.3 $\mu\text{g L}^{-1}$ using magnetic sector mass spectrometer, 0.13 $\mu\text{g L}^{-1}$ for nitrogen-phosphorous

***Corresponding author:** Kavita Arora, Advanced Instrumentation Research Facility, Jawaharlal Nehru University, New Delhi-110067, India, E-mail: kavitaarora@gmail.com, kavitaarora@jnu.ac.in

Received September 12, 2013; **Accepted** November 14, 2013; **Published** December 04, 2013

Citation: Singh A, Joshi Y, Choudhary M, Singh MP, Arora K (2013) Anti-atrazine Functionalized Gold-nano Structures for Environmental Monitoring. Biosens J 2: 105. doi: 10.4172/2090-4967.1000105

Copyright: © 2013 Singh A, et al. This is an open-access article distributed under the terms of the Creative Commons Attribution License, which permits unrestricted use, distribution, and reproduction in any medium, provided the original author and source are credited.

method and $2.4 \mu\text{g L}^{-1}$ using electron capture detection method [5]. The average quantification limit using these methods is $0.2 \mu\text{g L}^{-1}$ - $1.3 \mu\text{g L}^{-1}$. These methods are highly sophisticated methods that are highly sensitive but require high cost inputs, skilled technicians with complex/slow responsive features, which cannot be implemented for on-line monitoring. Until now, there is no single portable device available in the market that can efficiently detect low molecular weight toxic components (pesticides, herbicides etc.) in low cost [12]. The recent development of immunoassay techniques focused in most cases on decreasing analysis times, improving assay sensitivity, simplification and automation of the assay procedures, low-volume analysis for detection of low molecular weight pesticides. Immunoglobulin based biosensor (immunosensor) is an analytical opportunity which can be tailor-made to fabricate a device for hassle-free, on-site monitoring of desired analyte [13]. The selection of bio-element i.e. antibody integrated to a transducer collectively contribute to measure bio-recognition event and therefore, plays important role in immunosensor fabrication. Till date various immunosensors have been reported which mostly rely on optical and mass change phenomena [14,15]. However, electrochemical transducer provide advantages in terms of simplicity, reagent free, ease of miniaturization, easy tunability with the choice of wide range of suitable immobilization matrices and economical mass production [16]. Nano materials based immobilization matrices are available with unique properties that can be custom designed to suit the requirement. Liu et al. [17] developed electrochemical immunosensor using highly sensitive nanoparticle labels i.e., Quantum dots (QDs) of CdS@ZnS to detect prostate specific antigen (PSA) in spiked human serum sample via electrochemical stripping voltammetry having detection limit 20 pg mL^{-1} . Immunosensor was also able to detect human IgG upto 30 pg mL^{-1} within 7 minutes. Gold nano-particles coated carbon fiber microelectrode has been used to fabricate electrochemical immunosensor to detect carcino embryonic antigen up to 0.01 ng mL^{-1} using thionine doped magnetic nanospheres and HRP with in detection time of one hour through cyclic voltammetry [18]. Human serum IgG has been shown to be detected upto 5.0 pmol L^{-1} to

0.1 nmol L^{-1} using an immunosensor. This immunosensor combines anti-IgG immobilized onto ITO with double codified HRP doped nanoSiO₂ particles as labels with in detection time of one hour through cyclic voltammetry [19]. Ionescu et al. [20] developed electrochemical immunosensor based on poly nitrilo triacetic acid film electrogenerated onto gold electrode matrix combined to histidine tagged anti-atrazine (IgG) to detect atrazine in water sample. This immunosensor was able to detect upto 10 pg mL^{-1} in 80 minutes using impedance measurements. A gold nanoparticle coated nanocomposite of alkaline phosphatase and poly styrene-acrylic acid (PSA) nanospheres have been used to immobilize antibodies to fabricate an electrochemical immunosensor to detect tumor necrosis factor in human serum upto 0.01 ng mL^{-1} in 2 hours using differential pulse voltammetry [21]. This immunosensor retained 95% of its activity for one month when stored at 4°C [21]. Protein G magnetic beads (protein-G-MBs) fixed golmo di electrode has been used to immobilize anti-OA monoclonal antibody (anti-OA-MAb) for label free detection of okadaic acid upto $0.5 \mu\text{g L}^{-1}$ in around 1 to 2 hours using differential pulse voltammetry [22]. Gold nano-probes labeled with alkaline phosphatase conjugated secondary antibodies have been used to detect neuron specific enolase (NSE) in serum sample using anti -NSE coupled single-walled carbon nanotubes (NSE-SWNTs) onto glassy carbon electrode upto 0.033 ng mL^{-1} in 1 hour using DPV [23]. Myelo cytomatosis onco protein has been detected using immunosensor based onto gold substrate and gold nanopartiles labels in a sandwich assay in a linear detection range of 4.3 pmol L^{-1} to 43 n mol L^{-1} and detection limit 1.5 pmol L^{-1} in 1% serum sample using impedance spectroscopy [24]. Therefore, various immunosensors mentioned above have been summarized in Table 1. However, looking in to the applications of nanomaterials and need of an analytical device for atrazine, existing 'atrazine immunosensor' are separately mentioned in Table 2. It can be noticed here that majority of immunosensors reported in literature are based on labels to measure the bio-recognition event and require complex fabrication protocols leading to an immunosensor which is not stable beyond one month. Among these, gold nanoparticles based matrices have attracted

Matrix	Analyte	Redox indicator/label	Stability	Lowest detecting concentration	Response Time	Real sample	Ref.
Immuno-chromatographic strip	Prostate specific antigen(PSA)	Quantum dots(QDs, CdS@ZnS)	Long-term stability over a wide range of climates	30 pg mL^{-1}	7 min	Serum	[17]
IgG-FcD-ITO	p-aminophenol(AP)	Hydrazine	-	10 pg/mL	-	mouse IgG	[37]
antiCEA/pA/Au/CFME	carcinoembryonic antigen (CEA)	HRP	19 days at 4°C (retained 89.7% initial response)	0.01 ng/mL	1h	Serum	[18]
Ab/GNS/Chitosan/graphite/ carbon	carbohydrate antigens 153, 125, and 199(CA 153, CA 125, CA 199) and CEA	HRP	30 days at RT (>90% of initial responses)	Ranging from 0.084 to 16, 0.11 to 13, and 0.16 to 15 U mL^{-1} and 0.16 to 9.2 ng mL^{-1}	Less than 5 min	CA 153, CA 125, CA 199 and CEA	[36]
anti-IgG-SiO ₂ -HRP	human serum IgG	HRP	32 days at 4°C (retained 89.1% of its initial response)	5.0 pmol/L to 0.1 nmol/L IgG	~1h	plasma	[19]
IgG /CuCl ₂ /polyNTA	Atrazine	Histidine	After 30 min (RSD 10%)	10 pg mL^{-1}	~80	Water	[20]
Ab/ PANa/ GCE	TNF- α	Alkaline Phosphatase-Ab2-AuNPs/PSA	30 days at 4°C (more than 95% of its initial response was retained)	0.01 ng/mL	~2 h	Serum	[21]
Ab- Au-protein G magnetic beads	Okadaic acid	Label free	two weeks at 4°C without any loss	$0.5 \mu\text{g L}^{-1}$	~1 to 2 h	mussel	[22]
NSE-SWNTs-GCE	neuron specific enolase	AP-anti- IgG/ AuNPs	-	0.033 ng mL^{-1}	~1 h	Serum	[23]
AuNP-C _{AB} /C _{AG} /C _{AB}	Myelocytomatosisoncoprotein	AuNPs	-	1.5 pmol L^{-1}	-	1.5 pmol L^{-1}	[24]

Table 1: Comparative of various immunosensors reported in literature.

increasing attention due to their unique properties such as high biocompatibility, non-toxicity, tunable electronic and optical behavior, good conductivity and high catalytic activity. This has made nano-gold as a fundamental building block for the development of innovative functional material and that several novel strategies have been proposed to develop electrochemical immunosensors with high sensitivity using gold nanoparticles [25,26] (Table 1).

Scheme 1: Stepwise fabrication process for atrazine immunosensor for environmental monitoring

Present work focuses on application of electrochemically deposited gold-nano-structured indium tin oxide coated glass plates for fabrication of immunosensor for detection of atrazine (Scheme 1). Gold nano-structured film has been deposited onto ITO surface using a simple and one step process avoiding use of toxic ions through auric chloride solution at physiological pH and to decrease the cost of fabrication onto Indium tin oxide (ITO) coated glass plates [27-30].

Materials and Methods

Chemical and reagents

Hydrogen aurochloride (HAuCl_4), 1-ethyl-3-(3-dimethylaminopropyl) carbodiimide hydrochloride (EDC), N-hydroxysuccinimide (NHS), 11-mercaptoundecanoic acid (MUA), Na_2HPO_4 , KH_2PO_4 , NaCl, $\text{K}_3\text{Fe}(\text{CN})_6$, $\text{K}_4\text{Fe}(\text{CN})_6$, ethanol (EtOH), acetone, atrazine, ITO glass slides, Ag/AgCl, Pt wire etc. have been purchased from Sigma Aldrich. All experiments have been carried out using MB grade water from HI-Media. Rabbit monoclonal Anti-atrazine antibodies have been obtained from Thermo Scientific.

Measurement and apparatus

Three electrode electrochemical cell consisting of Ag/AgCl as reference electrode, Pt wire as counter electrode and ITO coated glass slide (0.6 cm×0.8 cm) as working anode has been used for all electrochemical measurements (cyclic voltammetry-CV; square wave voltammetry-SWV) using Autolab Eco Chemie, The Netherlands. FT-IR measurements have been carried out using Varian FT RAMAN, UV visible studies using Varian Carry 100 and SEM pictures have been taken using Zeiss EV40.

Electrodeposition of gold nano structures (GNS) onto ITO electrode

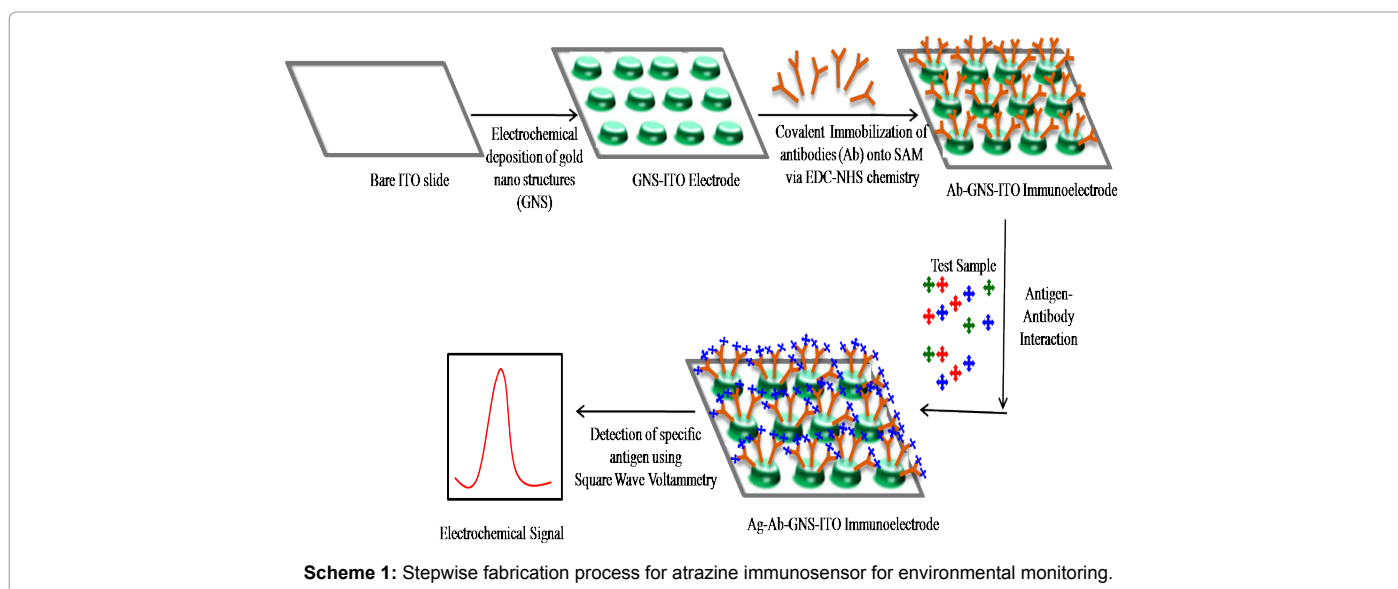
The ITO glass (0.6 cm×0.8 cm) was sequentially pre-cleaned via ultra-sonication using acetone, ethanol and distilled water, respectively, for 20 min each. Gold layer was electrochemically deposited using cyclic voltammetry in three electrode electrochemical cell containing 0.1 mM HAuCl_4 solution in 50 mM phosphate buffer solution (pH 7.5) at $55 \pm 2^\circ\text{C}$ for 30 cycles at 50 mVs^{-1} . The same electro-analyte solution was reused to deposit nano-structure gold (GNS) onto 5 ITO electrode surfaces providing uniform and satisfactory GNS-ITO to facilitate economies of cost. The fabricated gold layer was characterized using cyclic voltammetry, square wave voltammetry, UV-VIS spectrophotometry, FT-IR, SEM etc.

Fabrication of atrazine immunosensor (Ab-GNS-ITO)

GNS-ITO glass electrode was immersed in 5 mM mercaptoundecanoic acid (MUA) in ethanol for 2 h to have organic self-assembled monolayer (SAM) onto GNS surface to facilitate covalent immobilization of anti-atrazine (Ab). This MUA-GNS-ITO

Elements	Bare ITO (wt %)	GNS-ITO (wt %)	Ab-GNS-ITO (wt %)
In	1.23	0.98	0.86
Sn	0.85	0.76	0.72
Au	0	0.88	0
C	0.73	0.78	1.12
N	6.39	6.41	11.24

Table 2: EDX studies.



was exposed to EDC (50 mM) and NHS (10 mM) for 15 minute to convert the terminal carboxyl group on gold surface to an active NHS ester such that antibodies (anti-atrazine, Ab) can be immobilized [31]. 30 μ L of anti - atrazine (0.5 ng/mL) was spread over the GNS-ITO surface and kept for 2 h for Ab immobilization. Subsequently excess unbound antibodies were removed by rinsing with 10 mM PBS. The fabricated Ab-GNS-ITO electrode was then characterized using CV, SWV, FTIR, UV-VIS spectrophotometer, SEM etc. The Ab-GNS-ITO electrode was used to study the response characteristics for detection of atrazine using SWV in 0.05 M phosphate buffer pH 7.5. Ab-GNS-ITO electrode was exposed to desired concentration of antigen (atrazine) for 60 s and SWV measurements were taken after washing with PBS. Stability studies of the Ab-GNS-ITO electrode have been carried out.

Results and Discussion

GNS-ITO electrode

Wine red coloured GNS-ITO electrode was characterized using UV-visible spectroscopy and CV. Figure 1a shows UV visible studies of GNS- ITO electrodes with reference to bare ITO in reflectance mode using Varian Carry 100. It can be observed that characteristic peak at 559 nm can be ascribed to presence of nanostructure gold (20-30 nm range) deposited onto ITO surface [32]. It may be mentioned that this nanostructure gold can be hexagonally shaped. (Figure 1b) shows CV studies of bare ITO and GNS-ITO electrodes in Zobell's solution [5 mM $K_3Fe(CN)_6$ and 0.1M KCl]. It can be clearly seen that GNS-ITO shows considerable rise in peak currents (I_{pc} and I_{pa}) and decrease in peak

potential separation (E_p) to 0.166 V as compared to 0.221 V for bare ITO electrode (at 20 mV/s) revealing the improved electron transfer properties due to successful deposition of GNS (Figure 1b).

Scanning electron microscopic and EDX studies of Ab-GNS-ITO electrode

Figure 2 shows SEM images obtained for bare ITO, GNS-ITO, Ab-GNS-ITO electrode surface (Zeiss EVO40). SEM images obtained for GNS-ITO electrode surface (Zeiss EVO40) shows successful deposition of uniformly distributed spherical gold nano structures (GNS) onto ITO surface (Figure 2b) as compared to bare ITO surface (Figure 2a). These results are in agreement with the UV visible spectrum (Figure 1a). Presence of antibodies can be observed in (Figure 2c) for Ab-GNS-ITO electrode as the change granular morphology compared to GNS-ITO (Figure 2b) affirms the immobilization of antibodies onto GNS-ITO surface. These results have been further analysed using EDX spectroscopy and included in Table 2. The EDX results affirm that there is successful stepwise surface modification via clear indicatives for presence of Au (GNS-ITO) and then C and N for Ab-GNS-ITO electrode. Besides this it is worth mentioning that absence of Au for Ab-GNS-ITO surface is due to complete surface masking by antibody.

Electrochemical characterization Ab-GNS-ITO electrode

Figure 3a describes the CV characteristics of bare ITO, GNS-ITO, MUA functionalized GNS-ITO, Ab-GNS-ITO and Ab-GNS-ITO (surface blocked with BSA) electrode in Zobell's solution (5 mM

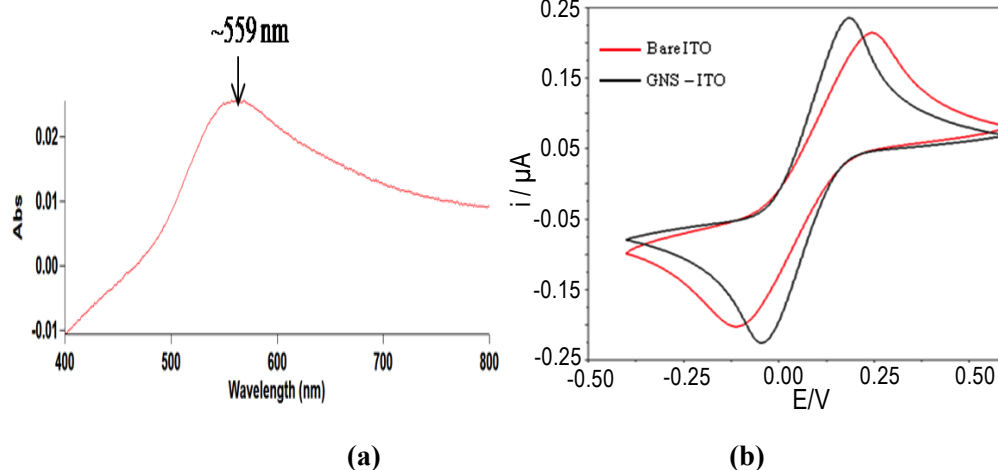


Figure 1: (a) UV-VIS spectroscopic studies of GNS-ITO electrode and (b) Cyclic voltammogram of bare ITO and GNS-ITO in Zobell's solution at 20 mV/s and temperature 25°C.

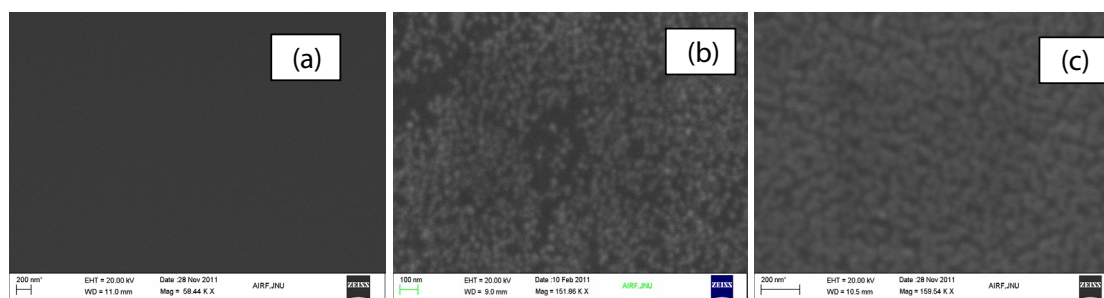


Figure 2: SEM images of (a) ITO, (b) GNS- ITO, and (c) Ab-GNS-ITO surface (Using Zeiss EVO40).

$K_3Fe(CN)_6$ in 0.1 M KCl) at 100 mVs^{-1} , 25°C . CV curve shows that increase in peak current has been observed for GNS-ITO surface (Curve ii) compared to bare ITO (Curve i) revealing increased rate of electron transfer. Further, MUA functionalized GNS-ITO surface (Curve iii) shows decrease in peak current indicate declining electron transfer rate that can be attributed to surface masking (due to compactly arranged self assembled monolayer of MUA). Subsequent decrease in peak current for Ab-GNS-ITO surface (Curve iv) affirms immobilization of bio-molecule (anti-atrazine antibodies) indicating presence of un-ionized protein at the surface [33]. Further decrease in peak current for BSA blocked Ab-GNS-ITO electrode once again confirms the phenomena of surface blocking by immobilized BSA (Curve v) [34]. Figure 3b, shows the characterization of bare ITO, GNS-ITO and Ab-GNS-ITO electrode using square wave voltammetry (SWV) in 10 mM PBS, pH 7.5 at 100 mV pulse amplitude and 25 Hz pulse frequency. The oxidation peak at 0.1 V observed for bare ITO electrode is attributed to the desorption of H^+ ions present on hydrolysed ITO surface. SWV studies of fabricated GNS-ITO electrode in PBS reveals that presence of oxidation peak at $\sim 0.78\text{ V}$ is obtained due to the formation of soluble Au (III) chloride complexes indicating successful deposition of nano-structured gold onto ITO surface [35]. The intensity of the peak height of similar peak decreased significantly for Ab-GNS-ITO electrode indicating successful immobilization of anti-atrazine (GNS surface masking) which is in coherence to the CV studies. However, emergence of a new oxidation peak towards lower potential of about 0.2

V for Ab- GNS-ITO electrode is due to the electrochemical oxidation of electroactive residues (tyrosine and lysine) present in proteins which show specific electrochemical signals [36]. Since most of the interferents in real word samples are known to oxidize on or after 0.5 V, rest of all experiments have been carried out at lower potential of 0.2 V.

Fourier transform-infrared (FT-IR) studies

The FT-IR spectra of GNS-ITO, MUA functionalized GNS-ITO and Ab-MUA-GNS-ITO electrodes are shown in Figure 4. Peaks observed near 1627 cm^{-1} , 470 cm^{-1} are attributed to the presence of gold nano particles/structures for GNS-ITO electrode while peaks at 1727 cm^{-1} (C=O), 630 cm^{-1} (C-S) can be attributed to formation of SAM (mercaptoundecanoic acid) onto GNS-ITO surface. Peaks arising at 1666 cm^{-1} (amide I: C=O), 1551 cm^{-1} (amide II: N-H), 1227 cm^{-1} (ester linkage) confirming the presence of antibodies immobilized onto MUA-GNS-ITO electrode [37]. All these studies are in coherence with CV (Figure 3a) and SEM studies (Figure 2) [38].

Response studies of Ab-GNS-ITO electrode

The cyclic voltammetric response of Ab-GNS-ITO electrodes (Figure 5a) has been studied for detection of atrazine (1 nM for 60s), in Zobell's solution at 100 mVs^{-1} . A significant decrease in peak current has been observed after antigen exposure stating successful formation of antibody-antigen complex. This observation has been confirmed by SWV studies (Figure 5b) of Ab-GNS-ITO electrode in PBS (0.01

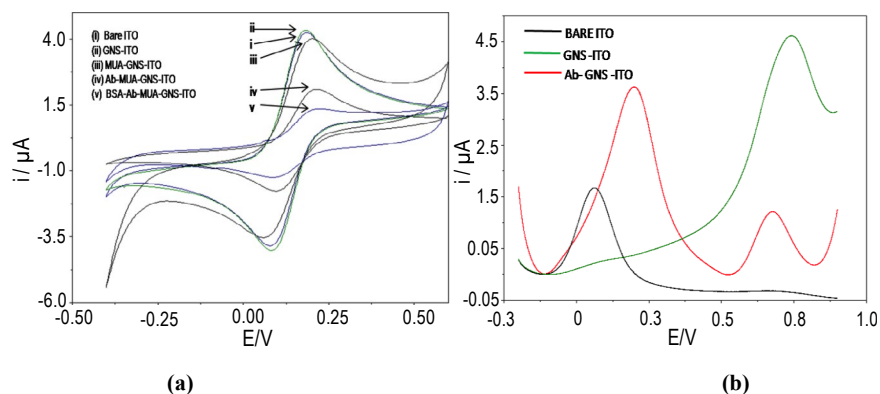


Figure 3: (a) Cyclic Voltammetric curves obtained at each step of modification in Zobell's solution at 100 mVs^{-1} ; (b) Square Wave Voltammetric curves of bare ITO, GNS-ITO, Ab-GNS-ITO electrode in 10 mM PBS, pH 7.5 at 100 mV pulse amplitude and 25 Hz pulse frequency.

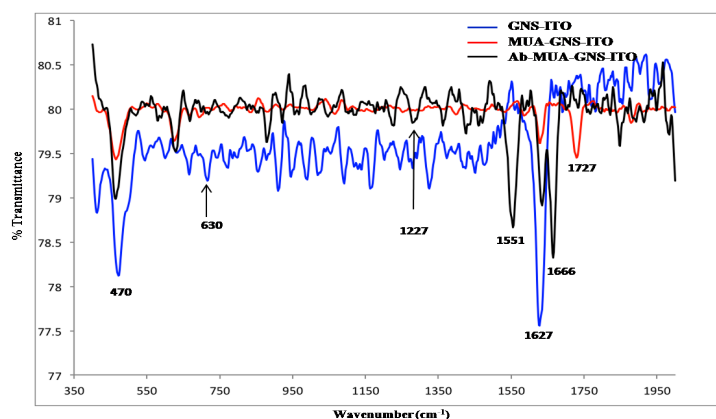


Figure 4: FT-IR spectra of GNS-ITO, MUA-GNS-ITO, Ab-GNS-ITO surface.

M), pH 7.4 at 50 mV pulse amplitude, 20 mV step potential, and pulse frequency of 25 Hz. The observed decrease in peak current can be attributed to the binding of antigen atrazine to the immunosensor electrode. Ab-GNS-ITO electrodes have been then subject to various concentrations of target analyte and the response characteristics have been described in Figure 6.

SWV Response studies of prepared Ab-GNS-ITO electrode (Figure 6a) indicate that peak current decreases with the increase in the atrazine concentration. It has been found that the immunosensor can detect atrazine in the linear range 50 aM to 1 nM (10.78 fg mL⁻¹-215 pg mL⁻¹). The decrease in peak current of immunosensor can be ascribed to the increase in electron transfer resistance of the electrode surface with increased concentration of analyte and thereby lowering the peak current [39]. Figure 6b, shows linear fit of obtained peak current (i) plotted with the logarithm of atrazine concentration (c) and the relationship can be described as (equation 1).

$$i (\mu A) = 1.93144 - 0.1914 \log c \quad (1)$$

The obtained coefficient of correlation, R²=0.99059. The lowest analyte concentration capable of bringing in change in the peak current of the immunosensor is 50 aM (10.78 fg mL⁻¹). This has been determined as the lowest concentration of analyte capable of bringing more than 5% change (decrease) in the peak current observed for Ab-GNS-ITO. Table 3 shows the comparison of the results obtained for Ab-GNS-ITO electrode with other reported atrazine immunosensors.

Specificity, stability and reusability studies of Ab-GNS-ITO electrode

Figure 7a describes the specificity studies of Ab-GNS-ITO electrode. SWV studies of Ab-GNS-ITO electrode have been carried out and peak current of the immunosensor have been plotted before and after exposure to 1 nM concentration of specific and non specific antigens.

It has been found that compared with the Ab-GNS-ITO electrode (A) peak current decrease only with the specific antigen atrazine (B) and no significant decrease was found with non specific antigens: malathion (C), 2-amino anthracene (D) and albendazole (E). This clearly indicates the fabricated immunosensor is highly specific to atrazine.

Figure 7b contains the stability studies of the prepared Ab-GNS-ITO electrode CV. CV measurement of freshly prepared Ab-GNS-ITO immunoelectrodes (A) were recorded and after washing electrodes were stored at 25°C and 4°C under desiccated conditions. It may be remarked that CVs of these immunoelectrodes recorded at an interval of 7 days exhibited 100% loss in the peak current at 25°C (E), while immunosensor retained about 90% signal up to 1st month followed by a gradual decrease in signal with 20% to 30% after 2nd and 3rd month at 4°C, respectively.

Reusability of Ab-GNS-ITO immunoelectrode has been estimated by dipping used electrode in 0.1 M NaOH. It is found that 5 min is sufficient to regenerate antibody molecules immobilized at Ab-GNS-ITO surface. These immunoelectrodes lose ~20% of the peak current after the sixth use (results not shown).

Conclusion

GNS-ITO electrodes have been successfully fabricated by unique, simple, nontoxic, direct electrodeposition method and have been used to develop a highly sensitive, cost effective immunosensor for detection of pesticide-atrazine. The prepared atrazine immunosensor (Ab-GNS-ITO immunoelectrode) is found to be specific for its specific analyte i.e. atrazine and was capable of detecting atrazine in the dynamic detection range of 50 aM⁻¹ nM (10.784 fg mL⁻¹ -215.68 pg mL⁻¹) with in 60 s antigen exposure time, at 25°C using SWV. The atrazine immunosensor showed consistent and sustained substantial response current for 4 weeks with 90% signal recovery upon reuse. The excellent performance of the immunosensor is attributed to large

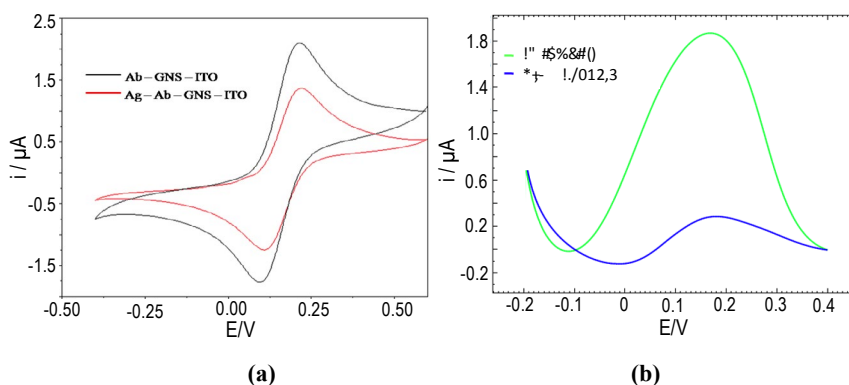


Figure 5: (a) Cyclic Voltammetric curves of prepared Ab-GNS-ITO electrode after its exposure to atrazine in Zobell's solution at 100 mVs⁻¹ and (b) Square Wave Voltammetric curves of Ab-GNS-ITO immunoelectrodes in PBS (0.01 M), pH 7.4 at 50 mV pulse amplitude, 20 mV step potential, and pulse frequency of 25 Hz after exposure to atrazine.

Sr. no	Matrix	Detection range	LOD of atrazine	Reference
1	Ab-K47/NP/PPY	0 ng mL ⁻¹ -170 ng mL ⁻¹	5 ng mL ⁻¹	[41]
2	anti-triazine biotinylated/neutravidin PPy/gold electrode	0.1-200 ng mL ⁻¹	0.1 ng mL ⁻¹	[42]
3	Ab-K47/magnetic beads/gold surface	10-600 ng mL ⁻¹	10 ng mL ⁻¹	[43]
4	Biotinyl K47H/ Neutravidin/Biotinyl-PE/MHDA/gold	10-300 ng mL ⁻¹	20 ng mL ⁻¹	[44]
5	Cu ²⁺ /histidine-tagged IgG atrazine antibody/PPy/NTA/gold	10 pg mL ⁻¹ - 1μg mL ⁻¹	10 pg mL ⁻¹	[20]
6	Anti atrazine-GNS-ITO	10.784 fg mL ⁻¹ -215.68 pg mL ⁻¹	10.784 fg mL ⁻¹	Present work

Table 3: Atrazine Immunosenors.

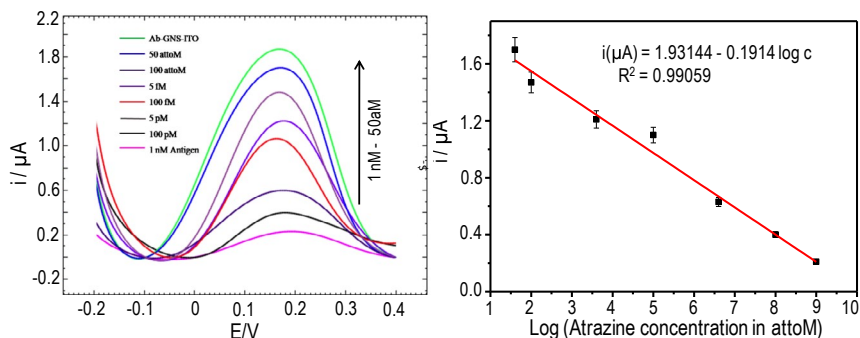


Figure 6: Square Wave Voltammetric curves of Ab-GNS-ITO immunoelectrode in PBS (0.01 M), pH 7.4 at 50 mV pulse amplitude, 20 mV step potential, and pulse frequency of 25 Hz after interaction with various concentrations of atrazine (50 aM, 100 aM, 5 fM, 100 fM, 5 pM, 100 pM, 1 nM); (b) Plot showing linear relationship between obtained peak current and logarithm of concentration of Atrazine.

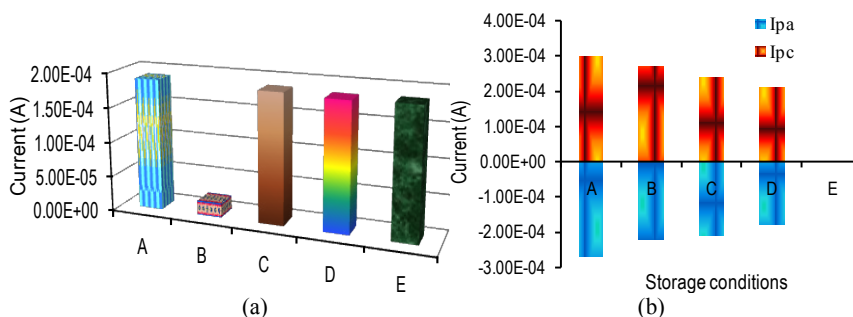


Figure 7: (a) Bar chart of peak currents of Ab-GNS-ITO electrode (A) exposed with 1 nM concentration of (B) atrazine, (C) malathion, (D), 2-amino anthracene, (E) albendazole, using square wave voltammetry in PBS (0.01 M), pH 7.4 at 50 mV pulse amplitude, 20 mV step potential, and pulse frequency of 25 Hz and (b) Bar chart of peak currents (Ipa and Ipc) obtained for freshly prepared Ab-GNS-ITO electrode (A), after 1st month (B), 2nd month (C), 3rd month (D) storage at 4°C and 7 days storage at 25°C (E) using cyclic voltammetry in Zobell's solution at 100 mVs⁻¹.

surface-to-volume ratio of spherical gold nano structures showing enhanced electrochemical activity and providing improved antibody immobilization. Additionally, presence of thread like MUA structure contributed facilitates the flexibility of antibody and increased the chances of interaction with atrazine. The findings of these investigations indicate enormous possibilities and implications towards the clinical diagnosis, food quality control and environmental monitoring for detection of different pesticide molecules.

Acknowledgement

We are grateful to Prof. Sopory, Vice Chancellor, Prof. Madhubala, Director, AIRF, JNU, New Delhi, India for their constant encouragement and infrastructural support. DBT sponsored projects IYBA-2008 (BT/B1/12/045/2008), RGYI-2009 (BT/PR13127/GBD/27/195/2009) and DST PURSE are dully acknowledged.

References

- About Pesticides (2010) U.S Environmental Protection Agency. Accessed.
- Kyle DJ (1985) The 32000 Dalton Qb Protein of Photosystem II, Photochem. Photobiol 41: 107-116.
- Bleidner WE, Baker HM, Levitsky M, Lowen WK (1954) Determination of 3-(p-chlorophenyl)-1,1-di- methyl urea in soils and plant tissue. J Agr Food Chem 2: 476-479.
- Schocken MJ, Speedie MK (1984) Physiological aspects of atrazine degradation by higher marine fungi. Archives of Environmental Contamination and Toxicology. 13: 707-714.
- Toxicological Profile for Atrazine (2003) Agency for Toxic Substances and Disease Registry (ATSDR), Department of Health and Human Services, Public Health Services. Atlanta, GA:US.
- Hallenbeck WH, Cunningham-Burns KM (1985) Pesticides and human health. Springer-Verlag New York.
- Hayes WJ, Laws ER (1990) Handbook of Pesticide Toxicology, Classes of Pesticides. Academic Press, Inc., New York, USA.
- Carabias MR, Rodriguez-G E, Herrero-H E, Sánchez-Ran Román FJ, Flores MGP (2002) Determination of herbicides and metabolites by solid-phase extraction and liquid chromatography: Evaluation of pollution due to herbicides in surface and ground waters. J Chromatogr 157-166.
- Lin CH, Lerch RN, Garrett HE, George MF (2007) Improved GC-MS /MS Method for Determination of Atrazine and Its Chlorinated Metabolites in Forage Plants-Laboratory and Field Experiments. Communications in Soil Science and Plant Analysis 38: 1753-1773.
- Giersch T(1993) A new monoclonal antibody for the sensitive detection of atrazine with immunoassay in microtiter plate and dipstick format. J Agric Food Chem 41: 1006-1011.
- Schneider P, Hammock BD (1992) Influence of the ELISA Format and the Hapten-Enzyme Conjugate on the Sensitivity of an Immunoassay for s-Triazine Herbicides Using Monoclonal Antibodies. J Agric Food Chem 40: 525-530.
- Marty JL, Garcia D, Rouillon R (1995) Biosensors: potential in pesticide detection. Trends in analytical chemistry 14: 329-333.
- Leca-Bouvier B, Blum LJ (2005) Biosensors for Protein Detection: A Review, Analytical Letters 38: 1491-1517.
- Satija J, Bharadwaj R, Sai V, Mukherji S (2010) Emerging use of nanostructure films containing capped gold nanoparticles in biosensors. Nanotechnol Sci Appl 3: 171-188.
- Pan H, Li D, Li J, Zhu W Fang L (2012) Enzyme-Mediated Growing Au Nanoparticles for Electrochemical and Optical Immunosensors: Signal-on and Signal-off. Int. J Electrochem Sci 7: 12883-12894.

16. Mallat E, Barceló D (2001) Immunosensors for pesticide determination in natural waters. *Trends in analytical chemistry* 20: 124-132.
17. Liu G, Lin YY, Wang J, Wu H, Wai CM, et al. (2007) Disposable electrochemical immunosensor diagnosis device based on nanoparticle probe and immunochromatographic strip. *Anal Chem* 79: 7644-7653.
18. Tang D, Yuan R, Chai Y (2008) Ultrasensitive electrochemical immunosensor for clinical immunoassay using thionine-doped magnetic gold nanospheres as labels and horseradish peroxidase as enhancer. *Anal Chem* 80: 1582-1588.
19. Zhong Z, Li M, Xiang D, Dai N, Qing Y, et al. (2009) Signal amplification of electrochemical immunosensor for the detection of human serum IgG using double-codified nanosilica particles as labels. *Biosens Bioelectron* 24: 2246-2249.
20. Rodica E, Ionescu Chantal G, Laurent B, Nicole Jaffrezic-R, Claude M, Serge Cosnier et al. (2010) Label-free impedimetric immunosensor for sensitive detection of atrazine. *Electrochimica Acta* 55: 6228-6232.
21. Yin Z, Liu Y, Jiang LP, Zhu JJ (2011) Electrochemical immunosensor of tumor necrosis factor α based on alkaline phosphatase functionalized nanospheres. *Biosens Bioelectron* 26: 1890-1894.
22. Hayat A, Barthelmebs L, Sassolas A, Marty JL (2012) Development of a novel label-free amperometric immunosensor for the detection of okadaic acid. *Anal Chim Acta* 724: 92-97.
23. Yu T, Cheng W, Li Q, Luo C, Yan L, et al. (2012) Electrochemical immunosensor for competitive detection of neuron specific enolase using functional carbon nanotubes and gold nanoprobe. *Talanta* 93: 433-438.
24. Jing-Lin He, Yan-Fei Tian, Cao Z, Zou W, Sun X (2013) An electrochemical immunosensor based on gold nanoparticle tags for picomolar detection of c-Myc oncoprotein. *Sensors and Actuators B: Chemical* 181: 835-841.
25. Liang R, Qiu J, Cai P (2005) A novel amperometric immunosensor based on three-dimensional sol-gel network and nanoparticle self-assemble technique. *Analytica Chimica Acta* 534: 223-229.
26. Ballarin B, Cassani MC, Maccato C, Gasparotto A (2011) RF-sputtering preparation of gold-nanoparticle-modified ITO electrodes for electrocatalytic applications. *Nanotechnology* 22: 275711.
27. Richardson JN, Osisek AJ, Dyer AL (2003) Spectro electrochemical Measurements at Colloidal Au Multilayer Optically Transparent Electrodes. *Electroanal* 15:1567-1570.
28. Dahanayaka DH, Wang JX, Hossain S, Bumm LA (2006) Optically transparent Au{111} substrates: flat gold nanoparticle platforms for high-resolution scanning tunneling microscopy. *J Am Chem Soc* 128: 6052-6053.
29. Kasmi AE, Leopold MC, Galligan R, Robertson RT, Saavedra SS, et al. (2002) Adsorptive immobilization of cytochrome c on indium/tin oxide (ITO): electrochemical evidence for electron transfer-induced conformational changes. *Electrochem Commun* 4: 177-181.
30. Wang L, Mao W, Ni D, Di J, Wu Y, et al. (2008) Direct electrodeposition of gold nanoparticles onto indium/tin oxide film coated glass and its application for electrochemical biosensor. *Electrochemistry Communications* 10: 673-676.
31. Shervedani RK, Hatefi-Mehrdadi A (2007) Electrochemical characterization of directly immobilized glucose oxidase on gold mercaptosuccinic anhydride self-assembled monolayer. *Sensors and Actuators B*, 126: 415-423.
32. Hu J, Wang Z, Jinghong Li (2007) Gold Nanoparticles With Special Shapes: Controlled Synthesis, Surface-enhanced Raman Scattering, and The Application in Biodetection. *Sensors* 7: 3299-3311.
33. Atchley DW, Nichols EG (1925) The influence of protein concentration on the conductivity of human serum. *J Biol Chem* 65: 729-734.
34. Chen X, Wang Y, Zhou J, Yan W, Li X, et al. (2008) Electrochemical impedance immunosensor based on three-dimensionally ordered macroporous gold film. *Anal Chem* 80: 2133-2140.
35. Eriksson K, Palmgren P, Nyholm L, Oscarsson S (2012) Electrochemical synthesis of gold and protein gradients on particle surfaces. *Langmuir* 28: 10318-10323.
36. Fredj HB, Helali S, Esseghaier C, Vonna L, Vidal L, et al. (2008) Labeled magnetic nanoparticles assembly on polypyrrole film for biosensor applications. *Talanta* 75: 740-747.
37. Singh S, Solanki PR, Pandey MK, Malhotra BD (2006) Covalent immobilization of cholesterol esterase and cholesterol oxidase on polyaniline films for application to cholesterol biosensor. *Anal Chim Acta* 568: 126-132.
38. Wang MS, Palmer LB, Schwartz JD, Razatos A (2004) Evaluating protein attraction and adhesion to biomaterials with the atomic force microscope. *Langmuir* 20: 7753-7759.
39. Liu X, Duckworth PA, Wong DKY (2010) Square wave voltammetry versus electrochemical impedance spectroscopy as a rapid detection technique at electrochemical immunosensors. *Biosensor and Bioelectronics* 25: 1467-1473.
40. Wu J, Yan Y, Yan F, Ju H (2008) Electric Field-Driven Strategy for Multiplexed Detection of Protein Biomarkers Using a Disposable Reagentless Electrochemical Immunosensor Array. *Anal Chem* 80: 6072-6077.
41. Esseghaier C, Helali S, Ben Fredj H, Tlili A, Abdelghani A (2008) Polypyrrole-neutravidin layer for impedimetric biosensor. *Sensors and Actuators B: Chemical* 131: 584-589.
42. Helali S, Martelet C, Abdelghani A, Maaref MA, Renault NJ (2006) A disposable immunomagnetic electrochemical sensor based on functionalised magnetic beads on gold surface for the detection of atrazine. *Electrochimica Acta* 51: 5182-5186.
43. Hleli S, Martelet C, Abdelghani A, Burais N, Jaffrezic-Renault N (2006) Atrazine analysis using an impedimetric immunosensor based on mixed biotinylated self-assembled monolayer. *Sensors and actuators B- Chemical* 113: 711-717.